



**EFFECTS OF CARBON CONTENT IN FERRITE
AND MARTENSITE ON LATTICE PARAMETER
AND ITS DIFFUSION PROCESS
(COMPUTER SIMULATION)**

By
Yilma Mengistu

A THESIS SUBMITTED TO THE SCHOOL GRADUATE STUDIES OF ADDIS ABABA
UNIVERSITY IN PARTIAL FULFILLMENT OF THE REQUIREMENTS FOR THE DEGREE OF
MASTER OF SCIENCE IN MATERIALS SCIENCE

AT
ADDIS ABABA UNIVERSITY
ADDIS ABABA, ETHIOPIA
JANUARY 2011

ADDIS ABABA UNIVERSITY
GRADUATE STUDIES

*EFFECTS OF CARBON CONTENT IN FERRITE AND MARTENSITE
ON LATTICE PARAMETER AND IT'S DIFFUSION PROCESS
(COMPUTER SIMULATION)*

By: Yilma Mengistu
Materials Science Program
Collage of Natural Science

Approved by the Examining Board

Dr. Mulugeta Bekele
(Advisor)

Dr. Ahmed M. Mohammed
(Examiner)

Prof. Teketel Yohannes
(Examiner, Chairperson)

Acknowledgements

Above all, I would like to thank the almighty; God, for letting me accomplish this stage.

I am deeply indebted to Dr. Mulugeta Bekele, my advisor, for his many suggestions and support and friendly approach during this research. My strongest thank is addressed to Dr. S.K Goshhal and Dr. Ahmed for their consistent support. I am also thankful to my Family and my intimate Friends for their support. Finally; I wish to thank the head of the program for his tireless follow up, support and advice.

Table of Contents

Table of Contents	iii
List of Tables	iv
List of Figures	v
Abstract	vi
1 Introduction	1
2 ATOMISTIC SIMULATION TECHNIQUE	11
2.1 Molecular Static Simulation	12
2.2 Molecular Dynamics Simulation	13
2.2.1 Equation of Motion	14
2.2.2 Method	16
2.2.3 Overview of Simulation program code	18
2.3 The Embedded Atom Method	20
2.3.1 Embedded Atom method potential for Fe-C	23
3 Model and Simulations Procedures	25
3.1 Molecular Static Simulation	25
3.1.1 Computational Procedures	26
3.2 Molecular Dynamics Simulation	29
3.2.1 Computational Procedure	30
4 Result and Discussion	32
4.1 Molecular Static Simulation Results in Ferrite	32
4.1.1 Determination of Preferential Position	32
4.2 Molecular Dynamics Simulation Results	37
4.3 Molecular Static Simulation Results in Martensite	42
5 Summary And Conclusion	45
References	47

List of Tables

3.1	Sample simulation box size.	26
3.2	Sample carbon concentration in ferrite (wt %).	29
4.1	Results of interstitial defect formation energies (E_f) at 300 K.	33
4.2	Comparison of simulation results of formation energies of carbon atom with Ab initio and experimental values at 300 K.	33
4.3	Result of migration and activation energies at room temperatures.	36
4.4	Results of equilibrium lattice constants (a) and (c) at room temperature.	37
4.5	Comparison of simulation results of minimum amount of carbon with ex- perimental values at 300 K.	38
4.6	Results of α and β compared with theoretical value.	41
4.7	Results of formation energies of carbon in martensite.	42
4.8	Results of migration energies of carbon in ferrite and martensite parallel and perpendicular to c-axis.	42

List of Figures

1.1	(A) body centered cubic structure of ferrite. (B) Tetragonal structure of martensite.	4
1.2	Preferential position of interstitial (A) octahedral positions and (B) tetrahedral positions.	5
1.3	Interstitial diffusion in metals.	7
1.4	Migration energy versus displacement curve when an interstitial diffuse from position 1-3	8
3.1	Simulation block of carbon introduced at octahedral position.	27
3.2	Simulation block of carbon introduced at tetrahedral position.	28
4.1	Plot of displacement versus reaction coordinate for carbon jump from one octahedral to the next octahedral position at 300 K.	34
4.2	Plot of displacement versus reaction coordinate for carbon jump from octahedral to tetrahedral position at 300 K.	35
4.3	Plot of migration energy versus temperature.	36
4.4	Plot of simulation result of lattice parameter versus carbon content at 300 K.	38
4.5	Plot of experimentally determined result lattice parameter versus carbon content at 300 K.	39
4.6	Plot of lattice parameter versus carbon content as a function of temperature.	40
4.7	Plot of square of displacement versus time at 300 K.	41
4.8	Migration energy curve of carbon in martensite and ferrite.	44

Abstract

Molecular dynamics and molecular static simulation has been performed to investigate the structural transition of martensite and the diffusion properties of single carbon atom in the bulk of ferrite. For both types of simulations embedded atom potential was applied to describe atomic interaction. This potential considers short-range interaction of iron and non-interacting defects which can be valid only for small concentration. After carrying out molecular static simulation we found that octahedral sites are the preferential position of carbon that have lowest formation energy -6.277 eV with minimum energy configuration than tetrahedral sites which have -5.349 eV formation energy. The migration energy of carbon calculated using this method when carbon moves from one preferential position to the next preferential position is 0.89 eV. This result is in good agreement with Ab initio calculation of migration energy 0.90 eV and experimental results 0.83 eV. From direct molecular dynamics simulation result of equilibrium lattice constant at room temperature we found that ferrite that contains carbon less than 0.081 wt % have cubical structure (that have equal values of lattice constant in the three direction (100), (010) and (001)). When the amount of carbon contained reaches 0.081 wt % the equilibrium lattice constant of martensite started splitting in to two values a and c. This splitting shows ferrite-martensite structural transition. Thus this content in our case is the minimum concentration (critical point) at which structural transition of martensite from body centered cubic to body centered tetragonal occur at room temperature. The diffusion coefficient calculated using molecular dynamic method is $9.736 \times 10^{-8} m^2/s$.

Chapter 1

Introduction

Most important for the properties of iron and steels are the contents and properties of impurities (defects) dissolved in iron. Carbon defect dissolved in iron plays an important role in the strength and toughness of steels, and has attracted a lot of attention for several decades until now. Crystal defects are imperfections that are found inherently in crystalline materials. By crystal defect one generally means any region where microscopic arrangement of ion differs drastically from the perfect one. The presence of defect affects physical, chemical, mechanical and electrical properties of the solid. Defects in crystal play an influential role in various technological processes and phenomena such as annealing, precipitation, diffusion, sintering, oxidation and others. Depending up on whether the imperfect region is bounded on the atom scale, all crystalline defects and imperfections can be classified in to four basic categories, such as point defects, line defects, plane defects and volume defects.

Point defects are imperfections which are not extended in space in any dimension. There is no strict limit for how small a “point” defect should be, but typically the term is used to mean defects which involve at most a few extra or missing atoms without an ordered structure of the defective positions. There are different types of point defects that can exist in the crystal. All of them are characterized by having atomic dimension in all direction.

A defect where an atom is missing from one of the lattice sites is known as a vacancy defect. It is the first types of point defects inherited to the crystal in equilibrium state. It is also called either Schottky or Frenkel defect. The former type of point defect is formed when an atom leaves its site (thereby creating a vacancy) and then moves to the surface of the crystal. In the latter case, the atom vacates its position in the lattice and transfers to an interstitial position in the crystal. The formation of Frenkel defect therefore creates two defects within the lattice (a vacancy and the interstitial) defect, while the formation of a Schottky defect leaves only one defect within the lattice (a vacancy).

Naturally vacancies occur in all crystalline materials at any temperature other than absolute temperature. At the melting point of some metals the concentration of defect can be approximately 0.1 % [1]. This means the imperfect crystal must have a lower free energy than does the perfect crystal.

The second types of point defect are formed when foreign atom whether it be an impurity or deliberate alloying addition, can occupy one of two distinct positions in the crystal. A solute substitute for an atom of the parent material (solvent) is said to be substitutional atom. And a solute that occupies a hole or interstice in the parent lattice is said to be interstitial atom. The occupancy of one of these two alternatives positions a solute atom takes depends on its size relative to the sizes of solvent atoms. The smaller the solute atom the most likely it exist as an interstitial and vice versa. In general in transition metals small defect atoms usually sits on interstitial site. There are two kinds of interstitial sites capable of accommodating small atoms. In bcc structure like ferrite the two types of interstitial sites are octahedral (o-sites) and tetrahedral (t-sites) sites.

Ferrite is one of the three allotropic forms of iron (δ , γ , and α). As molten iron cool down it crystallizes to body centered cubic (bcc) structured δ allotropes at about 1535 °c. Further cooling forms face centered cubic structured (fcc) γ -iron or austenite at 1394 °c and α -iron or ferrite (bcc) at 912 °c. The various properties of all forms of iron and

steels basically depend on the contents and properties of impurities (defects) formed during the process. Carbon, nitrogen and hydrogen are the typical interstitial defects that are found in pure iron and alloys (steel). Their presence plays a very important role to impart mechanical strength in these materials. Carbon and nitrogen dissolved in iron above their solubility limit are responsible for the formation of carbide and nitride which are very useful in improving strength, hardness and corrosion resistance of steel. The presence of H on the other hand may cause a lot of trouble by flaking, blistering, cracking and embrittlement of steels. Below the solubility limit the presence of even a very little amount of such impurities in interstitial position can have a drastic influence on the steel properties by increasing brittleness, and reducing weldability because of its tendency to form martensite steel as they build strong interaction with the lattice defect present.

Martensitic steels are similar to low alloy or carbon steels, having a structure similar to the ferritic steels. The main alloying elements are chromium, typically 12 to 15 %, molybdenum (0.2-1 %), and 0.1-1.2 % carbon. Their structures are “body-centered tetragonal” (bct) and they are classed as a “hard” ferro-magnetic group. It is formed by rapid cooling (quenching) of austenite which traps carbon atoms that do not have time to diffuse out of the crystal structure. This martensitic reaction begins during cooling when the austenite reaches the martensite start temperature (M_s) and the parent austenite becomes mechanically unstable. At a constant temperature below M_s , a fraction of the parent austenite transforms rapidly, and then no further transformation will occur. When the temperature is decreased, more of the austenite transforms to martensite. Martensite can also be formed by application of stress induced when the concentration of carbon in ferrite increases beyond the solubility limit. One of the differences between the two phases is that martensite has bct crystal structure, whereas ferrite has bcc structure. The transition between these two structures requires reorientation of iron atoms due to driving force (or concentration dependent shear strain).

The problem of phase transition of ferrite from body centered cubic to body centered tetragonal (martensite-transition) as shown in Fig 1.1 is associated with the amount and preferential position of carbon atoms dissolved in the solvent.

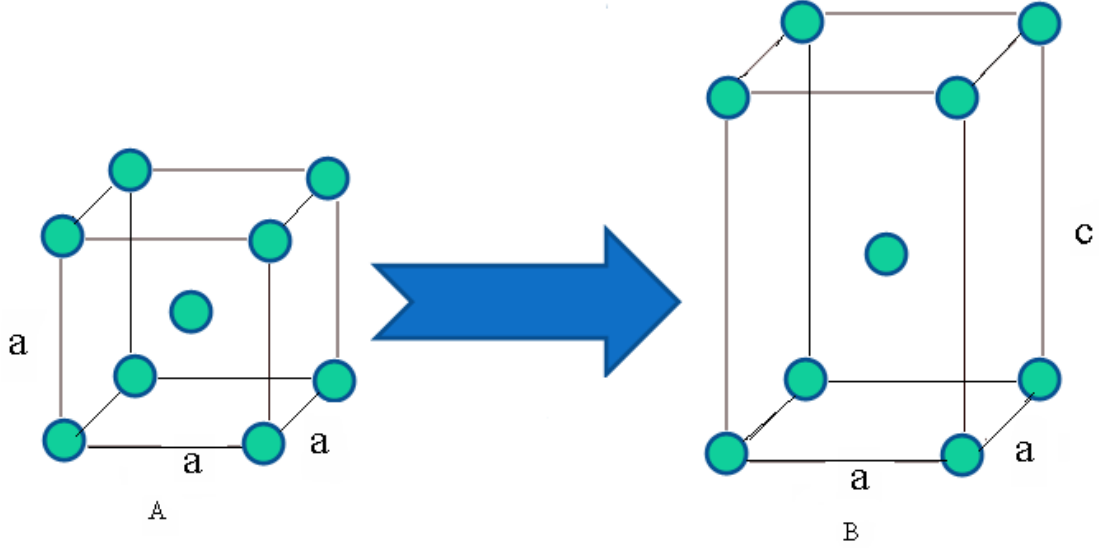


Figure 1.1: (A) body centered cubic structure of ferrite. (B) Tetragonal structure of martensite.

Similar to other interstitial defects carbon dissolved or introduced in the bulk of ferrite can occupy either of the two possible interstitial site mentioned above. In strain free bcc iron an o-site is found in the mid point of every pair of neighboring iron atoms oriented along one of the axis (100), (010) or (001) as shown in Fig 1.2 (A). A t-site is always found in the mid point of two adjacent octahedral sites as shown in Fig 1.2 (B). The alpha lattice has three octahedral interstitial sub lattice O_x , O_y and O_z displaced from the origin by the vector $h_1 = (0.5, 0, 0)$, $h_2 = (0, 0.5, 0)$ and $h_3 = (0, 0, 0.5)$ respectively. It is known that if the carbon atom occupies the three sub lattice uniformly the resulting lattice has cubic structure. The preferential occupation of one of the three sub lattice can therefore be viewed as an ordered distribution of carbon atom in them and this leads to the tetragonality of the resulting lattice [2]. In the early 1920s it was known that high carbon ferrous martensite is of tetragonal structure. Theoretically Zena [3] suggested that

the ordered distribution resulted from stress induced interaction of carbon. Thus there exists a critical carbon concentration at definite temperature above (or below) which ordering appears. This can be due to the resulting reduction in elastic energy dominates the decrease in entropy that leads to the decrease in free energy and this is the basic mechanism of phase transition.

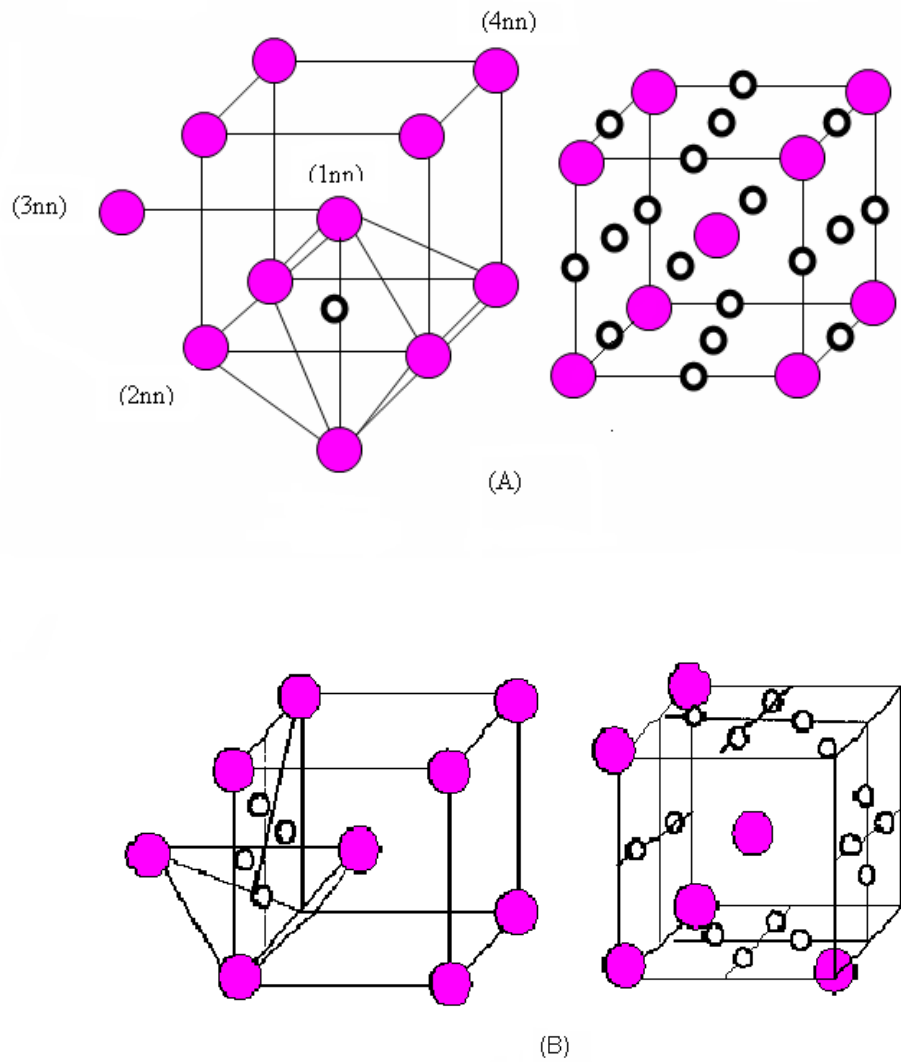


Figure 1.2: Preferential position of interstitial (A) octahedral positions and (B) tetrahedral positions.

The dependence of lattice parameter (a and c) (that determine structure) of martensite upon carbon content was established theoretically by Kurdjumov and Kaminsky [4] and latter these dependence was confirmed for high carbon concentration ≥ 0.56 wt % using a number of x-ray diffraction experiment by Hagg, Ohman, Honda and Nishlyama [5-8] etc. Several other isolated work predicted that tetragonality of martensite for carbon content as low as 0.2 wt % [9], 0.05 wt % [10] and 0.02 wt % [12]. Liu Xiao, Zhong [11] suggests their assumption for the cause of such variation. According to them this variation is because of different types of steel they used in their experiment (alloyed steel) and apparently some other effects arisen. On the other hand it was because at very low concentration the tetragonality splitting of x-ray diffraction peak is hidden by stress widening that makes difficult to get the value of a and c, Liu Xiao, Zhong Fan and Zhang Jinxia [11] applied the law of diffraction in their x-ray diffraction experiment studies to approximate the hidden peak for different specimen that contain carbon atoms in the range 0.0-0.79 wt %. And they found that 0.18 wt % of carbon concentration is the critical point at which structural transition of martensite from bcc to bct occurred at room temperature. Below the critical point carbon dissolved in ferrite has a cubic structure. D.E jiang and Emily A. carter [13] performed DFT calculation for ferrite carbon alloys with carbon dissolved at o-site and they have got saturation point of 0.17 wt %. Thus the value of the critical point at room temperature has been given theoretically with fluctuating results between 0.2 wt % and 0.5 wt %. The experimental values are also varies fluctuating between 0.18 wt % and 0.02 wt % owing to the difficulty of detecting low tetragonality and the self-tempering effects of low carbon martensite [14]. Despite diffusion of carbon in ferrite to occupy preferential position before stabilization, concentration dependence of the lattice parameter is the most important experimental proof of the fact that martensite is a super saturated solid solution of carbon in ferrite and the mechanism of transition is diffusionless homogeneous deformation [15].

Phase transformation (change of microstructure) in materials can be diffusion dependent, diffusion independent or diffusionless. Diffusion dependent phase transition is the first type that occurs when there is no change in composition (like melting and solidification) whereas diffusion independent transformation occurs when there is change in composition (eutectoid transformation). The transformation produced by cooperative small displacement of all atoms in the structure is diffusionless transformation. Atomic diffusion in crystals is usually mediated by point defects. The two basic mechanisms of atomic diffusion are vacancy mechanism and interstitial mechanism. However atoms located at the crystal lattice sites usually diffuse by a vacancy mechanism, while interstitial atoms diffuse by jumping from one interstitial site to the other interstitial site without displacing any of the matrixes as in Fig 1.3.

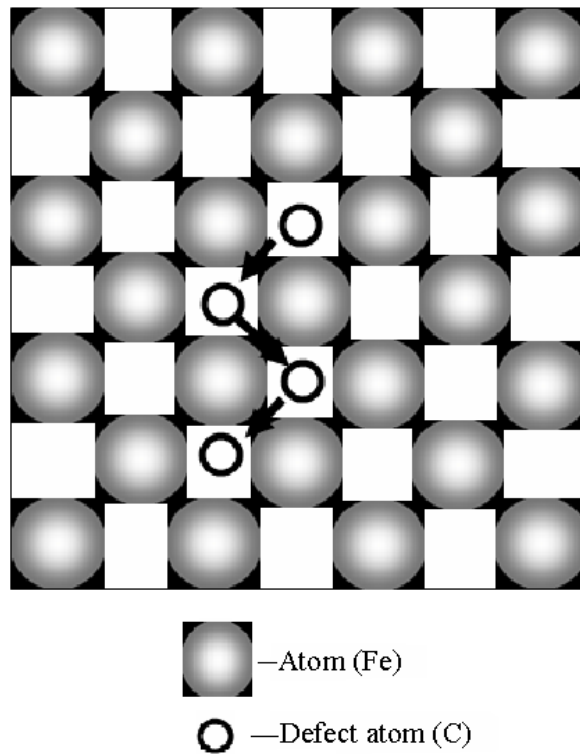


Figure 1.3: Interstitial diffusion in metals.

In both cases the atom must pass through a state of high energy and this creates an energy barrier as shown in Fig 1.4. Movement of carbon in iron is one example of interstitial diffusion. Since the energy requirement to squeeze most atoms (or ions) through a perfect crystal structure are so high (high energy barrier), diffusion is nearly impossible. Due to its relatively high diffusivity, interstitial diffusion of carbon often controls the kinetics of phase transformations in steels and the resulting microstructure. However, such diffusion may cause problems like strain aging, embrittlement, and steel erosion. Understanding the interstitial diffusion process in iron may help in understanding the behavior of steel subject to different environments.

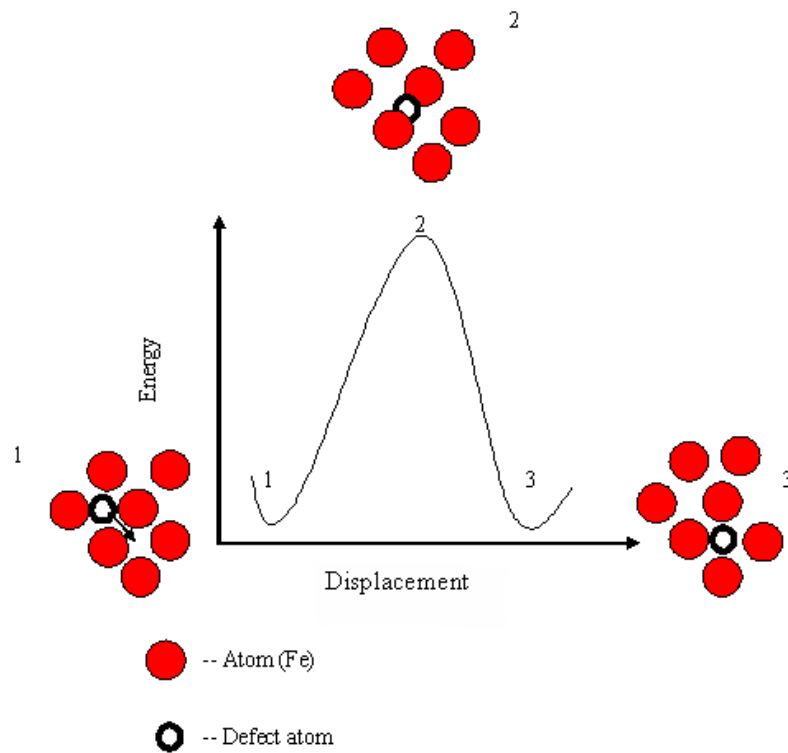


Figure 1.4: Migration energy versus displacement curve when an interstitial diffuse from position 1-3 .

In this work we have done molecular dynamics investigation using embedded atom potential (EAP) developed by D.J. Hepburn and G.J. Ackland [16] for small carbon concentration. Hepburn potential accounted for Fe-Fe and Fe-C interactions and neglect C-C interactions. There are some empirical potential that have been developed for ferromagnetic bcc α -iron containing carbon. Rosato's potential [17] is an empirical potential that include Fe-Fe and Fe-C interactions and neglect C-C interactions. Timothy T. Lau [18] and J. P. Perdew, K. Burke [19] potentials are many body potential that accounted for Fe-Fe, Fe-C interactions and Timothy potential neglect C-C interactions. Timothy's potential is an EAP developed using Finnis sinclair formalism [20] and J. P. Perdew's is an Ab initio potential. D. E. Jiang [13] and Ruda et al. [21] are EAP that includes C-C interactions, affording predictions of behavior for increased C concentrations. The Ruda et al [21] potential predicts that C occupies tetrahedral sites of a bcc iron lattice, whereas the other potentials favor the occupancy of octahedral sites.

Because of its technological importance the problem of martensite steel has been the focus of attention since very old time. For understanding the properties of ferrite martensite transition it is important to know the relation among the amount of carbon, preferential positions and diffusion process. In general this thesis aims to investigate the effect of carbon concentration on the structure of ferrite and study the diffusion characteristics of single carbon both in the bulk of ferrite and transformed martensite. Specifically using molecular static and molecular dynamic simulation techniques we planned to:

- a. Find the most stable preferential position of carbon in ferrite and martensite.
- b. Study the dependence of lattice parameter on concentration of carbon at two different temperatures 300 K and 1000 K and find the critical carbon concentration at which structural transition occurs.
- c. Study the diffusivity of carbon and its contribution for structural transition in the bulk of ferrite and martensite by calculating parameters that characterize diffusion before and after transformation.

The structure of this thesis is organized as follows. Chapter one is the introductory part in which the basic ideas related to ferrite-martensite transition is discussed. Chapter two introduces the molecular dynamics simulation method in general and overview of the particular software code (LAMMPS) used for this study. In chapter three we present the model and procedure of simulation in detail. The result of the simulation is reported in chapter four in two parts. In the first part the determination of preferential position and calculation of migration energy under molecular static frame work is presented. In the second part the variation of lattice parameter as function of carbon content at different temperature is discussed. Moreover the diffusion constant of carbon atom in ferrite is determined under molecular dynamics framework. In chapter five the summary and conclusion of the results obtained are presented.

Chapter 2

ATOMISTIC SIMULATION TECHNIQUE

The use of computer simulation techniques is becoming more and more important in the understanding of the microscopic behavior of materials. It is a very powerful toolbox in modern molecular modeling. It enables us to follow and understand structure and dynamics with extreme detail literally on scales where motion of individual atoms can be tracked. We carry out computer simulations in the hope of understanding the properties of assemblies of molecules in terms of their structure and the microscopic interactions between them. This serves as a complement to conventional experiments, enabling us to learn something new, something that cannot be found out in other ways. It acts as a bridge between microscopic length and time scales and the macroscopic world of the laboratory. We provide a guess at the interactions between molecules, and obtain ‘exact’ predictions of properties. The predictions are ‘exact’ in the sense that they can be made as accurate as we like, subject to the limitations imposed by our computer budget. At the same time, the hidden detail behind bulk measurements can be revealed. An example is the link between the diffusion coefficient and velocity autocorrelation function (the former easy to measure experimentally, the latter much harder). Simulations act as a bridge between theory and experiment. We may test a theory by conducting a simulation using the same model. We may test the model by comparing with experimental results. We may also carry out simulations on the computer that are difficult or impossible in the

laboratory (for example, working at extremes of temperature or pressure). Ultimately we may want to make direct comparisons with experimental measurements made on specific materials, in which case a good model of molecular interactions is essential. With the sophistication of the atomistic simulation methods and the increase of computational power, a more accurate description of the inter-atomic interactions in materials can be developed.

The two main families of simulation technique are molecular dynamics (MD) [22] and Monte Carlo (MC) [23]; additionally, there is a whole range of hybrid techniques which combine features from both. While MC, considered as a stochastic process, provides data such as diffusion coefficient, formation enthalpy or correlation factor, MD, considered as a determinist process, characterize the overall and physical behavior of the system. Because of the actual situation of the experimental techniques that do not allow an accurate description of the diffusion mechanisms, the computer simulations represent an appropriate tool. The present study was conducted with molecular static (MS) and MD calculations using embedded atom inter-atomic potentials.

2.1 Molecular Static Simulation

MS is a technique designed to determine the lowest energy configuration of a given system with and without the presence of defect. A three-dimensional simulation block is initially defined and minimized. Every atom within this block interacts with its surroundings as described by the given interaction potential. The presence of a defect induces forces on the atoms that are allowed to move in order to drive the system to a minimum energy configuration. This minimum energy state is reached through an iterative relaxation process. Using a conjugate gradient approximation method [24], the minimization technique moves the atoms along the direction of the steepest gradient of the energy function that is in the direction of greatest energy decrease.

In each single iteration step, the atom is displaced in the direction of the resultant force applied by its neighbors as well as in a direction perpendicular to its previous displacement. The energy is computed for each iteration and the system is assumed to be at equilibrium when the energy gradient drops to zero or when the forces on each atom are below a specified value. The number of iteration required to reach equilibrium may vary from several tens to several hundreds. This technique is however limited by the lack of temperature effect considerations. No atomic vibration due to thermal activation is taken into account and the results obtained only characterize the material at constant temperature.

2.2 Molecular Dynamics Simulation

MD is a form of compute simulation in which atoms and molecules are allowed to interact for a period of time by approximations of known physics, giving a view of the motion of the particles. This kind of simulation is frequently used in the study of microscopic properties of materials in materials science. This extremely powerful technique of molecular dynamics simulation involves solving the classical many-body problem in contexts relevant to the study of matter at the atomistic level. Since there is no alternative approach capable of handling this broad range of problems at the required level of detail, molecular dynamics methods have proved themselves indispensable in both pure and applied research. The advantage of MD simulations is that the simulations can be done with different statistical ensembles. Therefore, one can always specify the ensemble which corresponds to the experimental situation. Simultaneously one has an absolute time and temperature scale which allows immediate comparison with experiment. Molecular dynamics simulation consists of the numerical, step-by-step, solution of the classical equations of motion.

2.2.1 Equation of Motion

The behavior of a system of particles, including both electron and nuclei, can be determined by solving the time-dependent Schrödinger equation. The accuracy required by this type of approach yield to very complex calculations that make its application to the description of the system dynamics very difficult. Whereas a quantum mechanics analysis seems delicate to compute, a classical mechanics approach is relatively straightforward and provides useful information. Thus, MD is a technique that computes the equilibrium and the transport of a many body particle by solving the equation of motion of the system. If Newton's mechanics is sufficient to describe simple dynamics systems like atomic fluids, some more complex formulations such as the Lagrangian and the Hamiltonian [25] are necessary to deal with a more complex system. In the coming derivation, the Hamiltonian formulation is used to describe the fundamental concept of Molecular Dynamics. The classical Hamiltonian, H , can be identified as the total energy of a system, the combined kinetic and potential energies. For a system of N spherical particles the Hamiltonian can be written as:

$$H(p_i, r_i) = \frac{1}{2}m_i p_i^2 + \phi(r_i) \quad (2.2.1)$$

Where p_i is the momentum of a particle i ($p_i = m_i \dot{r}_i$, r being the position of the given particle and m_i its mass), and ϕ is the effective potential. The Hamiltonian is a function of $6N$ independent variables, the $3N$ momenta p_i and the $3N$ particle positions r_i . Considering an isolated system, the total energy E is conserved and the Eq. 2.2.1 is equal to a constant:

$$\frac{1}{2}m_i p_i^2 + \phi(r_i) = E = \text{const.} \quad (2.2.2)$$

Considering the total time derivative of the general Hamiltonian (Eq. 2.2.1) and a system that cannot exchange energy with its surrounding (Eq. 2.2.2), one can derive equations of motion for the particles of the system similarly to reference [26]:

$$\frac{dp}{dt} = \frac{\partial H}{\partial t} = \frac{\partial \phi}{\partial r} = f_i \quad (2.2.3)$$

$$\frac{dr}{dt} = \frac{\partial H}{\partial p_i} = \frac{p_i}{m_i} \quad (2.2.4)$$

Where f_i is the force applied to the particle i . Substituting Eq. 2.2.4 in 2.2.3, the Hamiltonian formulation yields Newton's second's law:

$$m_i \frac{dr^2}{dt^2} = f_i \quad (2.2.5)$$

Thus, Molecular dynamics consists essentially of integrating the equations of motions derived above via a numerical method. For very high accurate solutions of the equations of motion it is usually advantageous to solve a system of six first-order differential equations, as in the Hamiltonian approach (Eq. 2.2.1 and Eq. 2.2.2 applied in the three directions), rather than a system of three second-order differential equations as Newton's second law (Eq. 2.2.5 applied in the three directions). Based on this approach MD can be seen as a simulation of a system that evolves over a period of time where its particles moves in phase space along their physical trajectories as determined by the equations of motion.

2.2.2 Method

In a standard molecular dynamics simulation, general information about the system such as the number of atoms, the type, mass and atomic interactions are first defined. The initial configuration of the system, including the positions of the atoms and their initial velocities at the time $t = 0$, is then specified. The initial positions are obviously defined as a function of the crystallographic properties of the materials studied. The initial velocities are established as a function of a given initial temperature. Indeed, using a statistical thermodynamics approach, velocities can be computed from a temperature using the Maxwell-Boltzmann distribution. The value of the time step Δt corresponding to the integration variable, also has to be assigned before the simulation process starts. This value has to be low compared to the highest frequency motion to integrate accurately over the motions, but as large as possible to increase the length of the runs. The first step of the simulation corresponds to the calculation of the forces applied to the atoms at $t = 0$. Then, incrementing the value of Δt the actual positions, forces and velocities are successively computed for $t = t + \Delta t$, in integrating the equation of motion defined by Eq. 2.2.3 and Eq. 2.2.4 (or Eq. 2.2.5). The displacements of the atoms and their energies can then be calculated for $t = t + \Delta t$. This process is repeated until the number of iteration chosen is reached. The algorithm reported below illustrates the whole process described above.

- ◇ Composition of the system.
 - ♡ Define the number of atoms.
 - ♡ Define the type of atoms.
 - ♡ Define the specific masses of atoms.
 - ♡ Define the atomic interactions.
- ◇ Initial values of position and velocities at $t = 0$.
 - ♡ Assign the particles positions r_i .
 - ♡ Assign the particles velocities v_i .
 - ♡ Definition of a time step Δt .
- ◇ Simulation process (using the inter atomic potentials the force on this atom are calculated).
 - ♡ Initial force calculation at $t = 0$ (using this force the atomic positions and velocities are advanced through a small time interval Δt (time step)).
 - ♡ Calculate the position at $t + \Delta t$.
 - ♡ Calculate the force at $t + \Delta t$.
 - ♡ Calculate the velocities at $t + \Delta t$.
 - ♡ Time increment by Δt .
 - ♡ Analyze the results.

Scheme 2.1: Standard molecular dynamics algorithm.

2.2.3 Overview of Simulation program code

MD simulation is a useful technique to compute the equilibrium and the transport properties of a classical system. Considering that the MD algorithm is directly derived from a classical mechanics treatment of the system, the given system is expected to evolve as it would evolve during experiments. The approach is therefore very similar to real experiments. The sample is first prepared with a given structure specific atomic interactions. Then the sample evolves constrained to the equations of motion until its properties do not change with time. Since the MD technique follows the actual forces on the atoms as they migrate, the diffusion mechanisms can be determined by direct observation, without having any priori assumptions. The direct observations incorporate in a natural way correlation effects, entropy effects and other possible transformations in structure and/or mechanism that can occur with temperature. The relative importance of various mechanisms can also be studied as a result of the simulation. Thus, the MD simulation is a very powerful technique that yields to very detailed information about the simulated system. It is an appropriate tool when the goal is precisely study the exact nature of the diffusion mechanisms.

The MD computer program used to perform this study is LAMMPS 2009 version [27]. LAMMPS is a classical molecular dynamics code that models an ensemble of particles in a liquid, solid, or gaseous state. It can model atomic, polymeric, biological, metallic, or granular systems using a variety of force fields and boundary conditions. LAMMPS runs efficiently on single-processor desktop or laptop machines, but is also designed for parallel computers. LAMMPS was originally developed under a US Department of Energy CRADA (Cooperative Research and Development Agreement) between two DOE labs and 3 companies. It is freely-available molecular dynamics codes, distributed by Sandia National Labs. In most general sense, LAMMPS integrates Newton's equations of motion for collections of atoms, molecules, or macroscopic particles that interact via short- or long-range forces with a variety of initial and/or boundary conditions and for constant

number of particles (N), constant volume (V), constant energy (E), constant temperature (T) and constant pressure (P) using NVE, NVT, NPT integrators. All these integrators are set by a fix command that will be applied to a group of atoms. In LAMMPS, a "fix" is any operation that is applied to the system during time stepping or minimization. Examples include updating of atom positions and velocities due to time integration, controlling temperature, applying constraint forces to atoms, enforcing boundary conditions, computing diagnostics, etc. There are dozens of fixes defined in LAMMPS and new ones can be added. Force Fields supported include Amber, CHARMM, Dihedral, Embedded Atom Method based Force Fields and Class2 Force Fields (including cross terms).

In this work The molecular dynamics simulation of equilibrium lattice constant and mean square displacements are done using NPT integrator. It is time integrator which update the position and velocity of each atom in the group at each time step using Nose/Hoover temperature thermostats and Nose/Hoover pressure barostat (isothermal-isobaric ensemble) [28-30]. Thermostat and barostat integrators attempt to equilibrate the system to the requested target temperature and pressure specified by the user. Temperature is computed as kinetic energy divided by some number of degrees of freedom given by Eq. 2.2.6. And the pressure is computed by the formula given by Eq. 2.2.7.

$$T = \frac{\frac{1}{2}mv^2}{NK} \quad (2.2.6)$$

$$P = \frac{NK_B T}{V} + \frac{\sum_i^N r_i \cdot f_i}{dv} \quad (2.2.7)$$

Where N is the number of atoms in the system, K_B is the Boltzmann constant, T is the temperature, d is the dimensionality of the system (2 or 3 for 2d/3d), V is the system volume (or area in 2d), and the second term of Eq. 2.2.7 is the virial, computed within LAMMPS for all pair wise as well as 2-body, 3-body, and 4-body, and long-range interactions.

The energy minimization of the system is performed by iteratively adjusting atom coordinates under molecular static framework. Iterations are terminated when one of the stopping criteria such as stopping tolerance for energy and force are satisfied. There are two styles of minimization algorithm set by minimizer, Style-cg and Style-sd. Style-cg is the Polak-Ribiere (PR) version of the conjugate gradient (CG) algorithm. At each iteration the force gradient is combined with the previous iteration information to compute a new search direction perpendicular (conjugate) to the previous search direction. The PR variant affects how the direction is chosen and how the CG method is restarted when it ceases to make progress. The PR variant is thought to be the most effective CG. Style-sd is a steepest descent algorithm. At each iteration, the search direction is set to the downhill direction corresponding to the force vector (negative gradient of energy). Typically, steepest descent will not converge as quickly as CG.

2.3 The Embedded Atom Method

Many problems in materials science require a detail understanding of energetic and structure of non uniformities in metal and alloys. Due to the lower symmetries and long range strain generally found around defect the study of these problems requires techniques that can handle a large number of atoms. This in turn requires a model of a solid which is accurate and computationally simple. Historically these problems have been addressed with various pair potential model of energetic of the constituents of solid [31]. This approach is certainly useful in many circumstance. However there are some significant problems associated with the application of the pair potential with the local environments substantially different from the uniform bulk. This includes such a problem as surface, grain boundaries, internal voids and fracture processes. The use of density-independent pair potentials (the Lennard-Jones potential is a well-known example) is justified when the electron clouds responsible for the attractive and repulsive components of the inter-atomic interactions remain localized close to the individual atoms.

In metals this is no longer the case and valence electrons may be shared among atoms. These calls for potentials that take the local electron density into account and which, consequently, have a many-body nature. Daw and Baskes [32] have proposed an alternative to the pair potential approach based on density functional ideas which they called an embedded atom method (EAM). As with pair potential models the energetic of an arbitrary arrangement of atom can be calculated quickly but the ambiguity of the volume dependence inherent in pair potential mode [33] is avoided. This method has already been applied to several problems with good result. Within the frame work of density functional theory the total electron energy for an arbitrary arrangement of nuclei can be written as a unique functional of the total electron density. The starting point of the EAM is the observation that the total electron density in a metal is reasonably approximated by the linear super position of contribution from the individual atoms. The electron density in the vicinity of each atom can then be expressed as a sum of density contributed by the atom in question plus the electron density from all the surrounding atoms. This latter contribution to electron density is a slowly varying function of position. By making the simplification that this background electron density is constant, the energy of this atom is the energy associated with the electron density of the atom plus the constant background density of the atomic species. In addition there is an electrostatic energy contribution due to core-core overlap. It is based on the Hohenberg-Kohn theorem [34], which states that the energy contribution of an atom on its surrounding neighbors is a function of the local electron density due to all the surrounding atoms. This approach becomes particularly important when point defects such as vacancy clusters, free surfaces, grain boundaries or dislocation cores are introduced and change the density in the materials. Based on the EAM approach, the interaction energies of the atoms are composed of two potentials functions. A classical pair interaction potential describes the attractive and repulsive electrostatic interaction between two atoms.

An embedding function, F , takes into account the interaction energy of each atom with the local electron density associated with the neighboring atoms. Consequently, the total energy of the system is written as:

$$E_{tot} = \sum F_i(\rho_{h,i}) + \frac{1}{2} \sum_{i=j} \phi(R_{i,j}) \quad (2.3.1)$$

In this expression $(\rho_{h,i})$ is the host electron density at atom i due to the remaining atom of the system, $F_i(\rho_{h,i})$ is the energy to embed atom i in to the background electron density and $\phi(R_{i,j})$ is the core-core repulsion between atom i and j separated by the radius $R_{i,j}$. F_i depends only on atom i and $\phi(R_{i,j})$ only depends on the elements of atoms i and j . The electron density is approximated by the superposition of atomic densities.

$$\rho_{h,i} = \sum_{j=i} \rho_a(R_{i,j}) \quad (2.3.2)$$

Where ρ_a is the electron density contributed by atom j . Note that the embedding function F_i is universal in that it does not depend on the source of the background electron density. Thus the same embedding function is used to calculate the energy of an atom in an alloy that is used in the pure material. This universality makes the embedding atom method particularly appealing for studies of alloys. To apply this method the embedding function, pair repulsion and atomic densities must be known. The atomic densities will be taken from Hartree-Fock calculation [35]. Approximate values of the embedding functions and pair interaction can be calculated from the formal definition of this quantity within the density functional frame work as described by Daw [32]. These functions however only give qualitatively correct prediction of the material properties, it is necessary to determine this function empirically in order to obtain accurate description.

The embedding function F_i is calculated by assuming that the crystal obeys Rose's equation of state [36], who has shown that the sublimation energy of most metal as a function of lattice constant can be scaled to simple universal function.

$$E(a) = -E_{sub}(1 + a^*)e^{-a^*} \quad (2.3.3)$$

In this expression, E_{sub} is the absolute value of the sublimation energy at zero temperature and pressure. The quantity a^* is a measure of the deviation from the equilibrium lattice constant given by:

$$a^* = \left(\frac{a}{a_o} - 1\right) \left(\frac{9B\Omega}{E_{sub}}\right)^{\frac{1}{2}} \quad (2.3.4)$$

Here B is the bulk modulus of the material, a is a length scale characteristic of the condensed phase (bcc lattice constant for example), a_o is the equilibrium lattice constant and Ω is the equilibrium volume per atom. This expression has been shown to give a good fit to the equation of state of numerous metals.

2.3.1 Embedded Atom method potential for Fe-C

The EAM potentials (EAP) used in this study to simulate the martensite were developed by Derek J. Hepburn and Graeme J. Ackland [16]. It is developed by fitting experimental parameters using constant volume relaxation procedure at 0 K. The model incorporates the magnetic second moment tight-binding picture for iron, charge transfer from iron to carbon, and a covalent picture of localized Π -bonding around carbon atoms. The potential is suitable for large scale MD, being short-ranged and computationally equivalent to EAM. The formalism allows predicting the interactions between carbon and a range of defects in iron, many of which are intractable with conventional potentials. For the binding of carbon to over coordinated defects such as those present in grain boundaries and dislocations, and so represent an important test of potential transferability. The Ab initio data shows a strong repulsion between over coordinated defects and nearby carbon atoms. By contrast previous potentials all show strong binding.

Despite significant effort, they were unable to refit these potentials to reproduce this repulsion in addition to the other targets from their fitting database. Thus they conclude that it is the functional form of these potentials, not the parameterizations, which gives the binding. And their covalent-style potential has saturation of the carbon embedding function, which means that any extra nearby iron atoms do not give increased binding. Thus they were able to successfully fit the carbon self-interstitial energies by better describing the physics involved. All potentials and the ab initio data show positive binding between interstitials and carbon at separations where strain field effects are expected to dominate. This is consistent with experiment which shows a similar binding between carbon and a highly mobile point defect, and corroborates their interpretation that this defect is a self-interstitial around carbon atoms. The potential is suitable for large scale MD, being short-ranged and computationally equivalent to EAM. Having a good prediction of thermodynamics properties done using this potential in ferrite, In this work using this potential we tried to predict the critical amount of carbon content for martensitic transition and the diffusion characteristic as discussed before.

Chapter 3

Model and Simulations Procedures

In this chapter we discussed the model and simulation procedure of MS and MD techniques used to study the amount and diffusion characteristic of carbon in martensite transition. Molecular static simulation is used for two purposes. First it is used to determine the preferential position of carbon which is related to its stability and stability of the whole system. Secondly it is used to find the migration energies that characterize diffusion of carbon in the vicinity of ferrite and martensite. Molecular dynamic simulation in the other hand is performed to calculate the equilibrium lattice constants of Fe-C system for a numbers of samples that have different amount of carbon atoms introduced at the preferential position. In addition the rate of diffusion of single carbon atom is calculated using this method. The result of the simulation and related ideas are discussed in chapter four.

3.1 Molecular Static Simulation

The formation energy of defect is the difference between the minimum energy of simulation block with the given defect (E_{fd}) introduced at possible interstitial site and the minimum energy of the perfect block (E_p). Because the two systems do not have the same number of atoms, the formation energy is not simply the difference of minimum energy of the perfect crystal without defect and the minimum energy of crystal in the presence

of defect. This is because in the perfect crystal, all atoms contribute equally to the total energy and there would be extra contribution with the introduction of defect. Therefore, we expect the energy contribution of $N+1$ atoms in the perfect crystal structure to be $\frac{N+1}{N} \times E_p$. The formation energy of defect at the two possible interstitial sites, octahedral and tetrahedral can be computed from the following relations:

$$E_{fo} = E_o - E_p \frac{(N+1)}{N} \quad (3.1.1)$$

$$E_{ft} = E_t - E_p \frac{(N+1)}{N} \quad (3.1.2)$$

where E_{fo} and E_{ft} are carbon defect formation energies at octahedral and tetrahedral position respectively, and N is the number of iron atoms.

The effect of box size on the result of simulation was checked simultaneously by comparing the calculated formation energy for four sample boxes of different sizes all with periodic boundary condition shown in Table 3.1.

Table 3.1: Sample simulation box size.

<i>box dimension</i>	$10 \times 10 \times 10$	$11 \times 11 \times 11$	$15 \times 15 \times 15$	$20 \times 20 \times 20$
<i>number of atom contained</i>	2000	2662	6750	16000

3.1.1 Computational Procedures

The minimum energy of pure alpha iron E_p , (without defect) is calculated for perfect block of specific sample box with a periodic boundary condition at constant temperatures. Minimization of the system is performed using conjugate gradient relaxation method. The embedded atom potential that is used to describe the atomic interaction enables the relaxations of the surrounding Fe atoms up to the third nearest-neighbor. The relaxation is performed for 10^5 iterations until the system reach equilibrium at defined energy tolerance

of 10^{-8} . During minimization the dimension of the boxes varies in each iteration until the energy of the final configuration became minimum at the given condition. A single carbon atom is then introduced in the bulk of ferrite at the octahedral site as shown in Fig 3.1. After the system is relaxed in same way as before the minimum energy , E_o , of the structure with defect at these position is calculated.

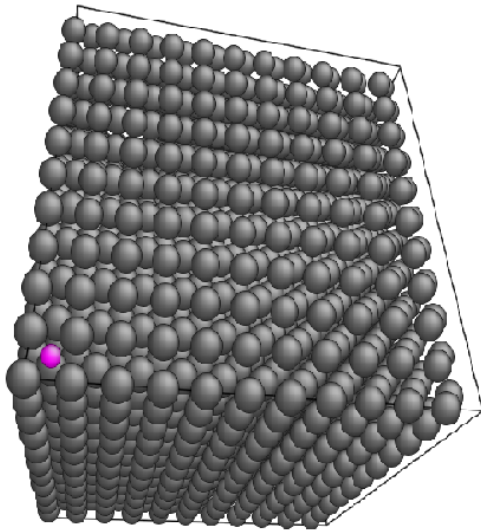


Figure 3.1: Simulation block of carbon introduced at octahedral position.

The minimum energy at tetrahedral site , E_t , is then calculated in the same way for carbon introduced at tetrahedral site as shown in Fig 3.2. Finally the formation energy of single carbon defect per atom at both sites is calculated using Eq. 3.1.1 and Eq. 3.1.2.

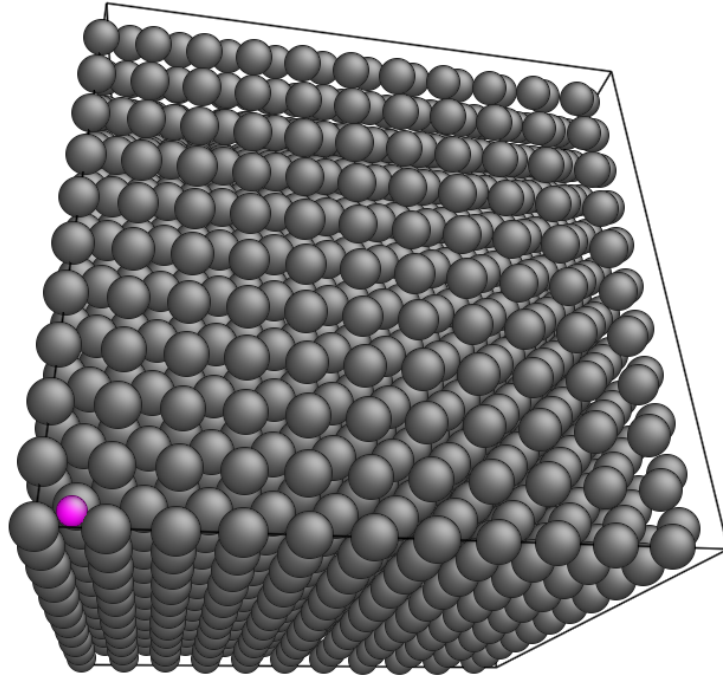


Figure 3.2: Simulation block of carbon introduced at tetrahedral position.

Diffusion assisted by interstitial defect is the migration from one interstitial position to adjacent empty one. In this process activation energy is required for a diffusing atom to squeeze past neighbor atoms to reach a new site. Activation energy (Q) of a given defect (carbon) is the sum of formation energy and migration energy (E_m). Migration energy of defect (carbon) is found by applying dragging method which is a suitable method of calculating minimum energy path for single particle migration in a crystal lattice. Using this method the minimum energy of carbon is obtained as a function of atomic displacement along the jump vector.

The maximum in this curve represents the saddle-point energy. This energy minus its initial energy before the jump is identified as the migration energy. To find these paths, single carbon atom introduced at octahedral position (1.5, 0.5, 1.0) is dragged step by step first towards the next t-site (1.75, 0.5, 1.0) and then towards the next nearest o-site (2.0, 0.5, 1.0) along (100) direction. Each step had a uniform step size of 0.1 lattice unit. At each step the total energy of the simulation box is minimized with respect to all other atom using conjugate gradient relaxation. The search for minimum is then carried out until the system equilibrates or attains local minima with energy tolerance of 10^{-8} for 10^5 iterations.

3.2 Molecular Dynamics Simulation

Molecular dynamics simulations of equilibrium lattice constants of each sample and diffusion coefficient of single carbon atom are calculated at constant temperature. For all molecular dynamics simulation discussed below we used a cubical block of dimension $11 \times 11 \times 11$ that contains 2662 mobile atoms with repeating periodic boundary conditions in the three vectors directions ((100), (010) and (001)). Inter atomic interaction between irons and iron and carbon are described by the EAM potentials as discussed before. The effect of amount of carbon on equilibrium lattice parameter that have equal value, a, in all the direction of the three vectors for bcc structure to split into two values, a, and, c, for bct are studied for specimen that contain increasing number of carbon atom shown in Table 3.2 below.

Table 3.2: Sample carbon concentration in ferrite (wt %).

<i>Number of carbon</i>	5	10	20	30	40	50
<i>concentration (wt %)</i>	0.0405	0.081	0.162	0.243	0.324	0.405

3.2.1 Computational Procedure

After a number of carbon atoms are introduced randomly in the bulk of ferrite at the preferential positions according to the number specified in the sample, MD simulation is performed for constant number of particle, pressure and temperature (that is the system is allowed to evolve until it equilibrate). This is time integration that update positions and velocities of each atom for every time step. During integration at each time steps the temperature and the pressure of the group are controlled by a Nose/Hoover temperature thermostat and Nose/Hoover pressure barostat respectively. This creates a system trajectory consistent with the isothermal-isobaric ensemble. The simulation is run for 10^5 molecular dynamic time steps until the system reaches equilibrium at zero pressure. The same time integrator is also used to perform molecular dynamics calculation of diffusion coefficient of a single carbon in ferrite in terms of mean square displacement using Einstein's relation (Eq. 3.2.1):

$$D = \lim_{t \rightarrow 0} \frac{\langle R^2 \rangle}{2nt} = \lim_{t \rightarrow 0} \frac{\langle |R(t) - R(0)|^2 \rangle}{2nt} \quad (3.2.1)$$

where the Dirac brackets $\langle \rangle$ indicate an average over a large number of particles and n is the dimensionality.

In Eq. 3.2.1 the diffusion coefficient is understood to be a tracer diffusion coefficient and the implication is that we can follow each particle explicitly. In this calculation energy conservation and stability of the simulated system over a long time are essential for diffusion studies. For this reason the simulation was performed for a time step of 10^7 for a time of 1ns which is found to be sufficient for the equilibration of the system as an NVE ensemble.

Diffusion rates usually characterized by the diffusion constant, D , which exhibits an Arrhenius temperature dependence Eq. 3.2.2.

$$D = D_o \exp \frac{-Q}{K_B T} \quad (3.2.2)$$

where D_o is the pre exponential factor, Q the activation energy, K_B Boltzmann constant and T is the temperature. The diffusion coefficient or pre exponential factor is computed from this relation.

Chapter 4

Result and Discussion

4.1 Molecular Static Simulation Results in Ferrite

This section contains molecular static simulation results of formation and migration energies in ferrite. Formation energies are obtained for a single carbon atom introduced at the two possible interstitial sites (o-site and t-site) of ferrite using Eq. 3.1.1 and Eq. 3.1.2 as discussed in Chapter three. The formation energies results are used to identify the preferential position of carbon in ferrite so that the effect of carbon concentration on lattice parameter (on structural transition) is investigated independently for all carbon atoms in specified samples found at their preferential positions. Moreover the comparison of preferential positions of carbon in ferrite and martensite are made to predict the nature of structural transition at constant temperature.

4.1.1 Determination of Preferential Position

The result of formation energies for each sample box size at the two possible interstitial sites are given in Table 4.1. As we can see the results from the table, for all sample box sizes the formation energies of carbon introduced at octahedral positions (E_{fo}) are less than the corresponding formation energies of carbon introduced at tetrahedral one (E_{ft}).

That is for all sample box sizes octahedral positions are energetically favored. This indicates that the system configuration has minimum energy when all carbon atoms introduced in the bulk of ferrite occupies octahedral positions. Therefore according to our simulation results of formation energies octahedral site is found to be the preferential positions where all carbon atoms in it reside at equilibrium. These result of formation energies we found using embedded atom potential and the conclusion we made are in good agreement with Ab initio and experimental results reported previously as shown in Table 4.2 [16-19].

Table 4.1: Results of interstitial defect formation energies (E_f) at 300 K.

<i>box size</i>	$E_p(eV)$	$E_o(eV)$	$E_t(eV)$	$E_{ft}(eV)$	$E_{fo}(eV)$	$(E_{fo}-E_{ft})(eV)$
$10 \times 10 \times 10$	-8025.963	-8032.129	-8030.709	-4.746	-6.166	-0.420
$11 \times 11 \times 11$	-10579.369	-10585.604	-10584.718	-5.349	-6.235	-0.886
$15 \times 15 \times 15$	-27087.626	-27093.762	-27092.762	-5.136	-6.136	-1.000
$20 \times 20 \times 20$	-64207.706	64213.837	-64212.843	-5.137	-6.131	-0.994

Table 4.2: Comparison of simulation results of formation energies of carbon atom with Ab initio and experimental values at 300 K.

<i>Result</i>	<i>This work (eV)</i>	<i>Timothy (eV) [16]</i>	<i>J.P.Perdew (eV) [19]</i>	<i>Rosato (eV) [18]</i>
E_{ft}	-5.35	-6.38	-6.25	-5.03
E_{fo}	-6.24	-7.15	-7.11	-6.14
$(E_{fo} - E_{ft})(eV)$	-0.89	-0.77	- 0.86	-1.11

Comparing the result of formation energies we obtained for the four box sizes shown in Table 4.1 we found that the variation of calculated energies for a cubical box size of dimension > 11 are not as such significant. For this reason both molecular static and molecular dynamic analysis for the rest of the simulation is done for a box size of $11 \times 11 \times 11$ with a periodic boundary condition.

The migration energy curve as a function of atomic displacement represented by Fig 4.1 and Fig 4.2 are obtained using dragging method under molecular static frame work. The first curve shows the migration (jump) of carbon atom from one octahedral position (1.5, 0.5, 1.0) to the next nearest neighbor octahedral position (2.0, 0.5, 1.0) via tetrahedral position. In this curve the local minimum energy of the system increases step by step with displacement up to the maximum then drops to a minimum in the direction of jump vector. The maximum in this curve corresponds to tetrahedral position (1.75, 0.5, 1.0). According to this the system have minimum energy configuration when carbon found in the interstitial of ferrite occupies octahedral position before and after jump.

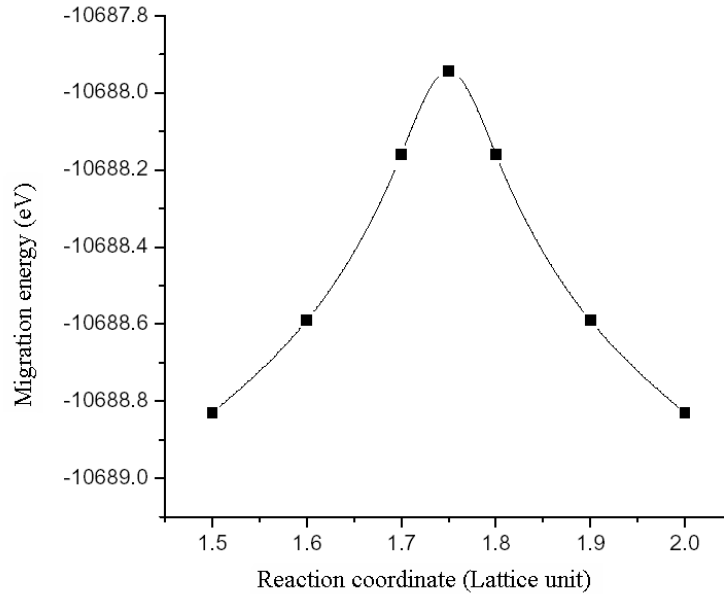


Figure 4.1: Plot of displacement versus reaction coordinate for carbon jump from one octahedral to the next octahedral position at 300 K.

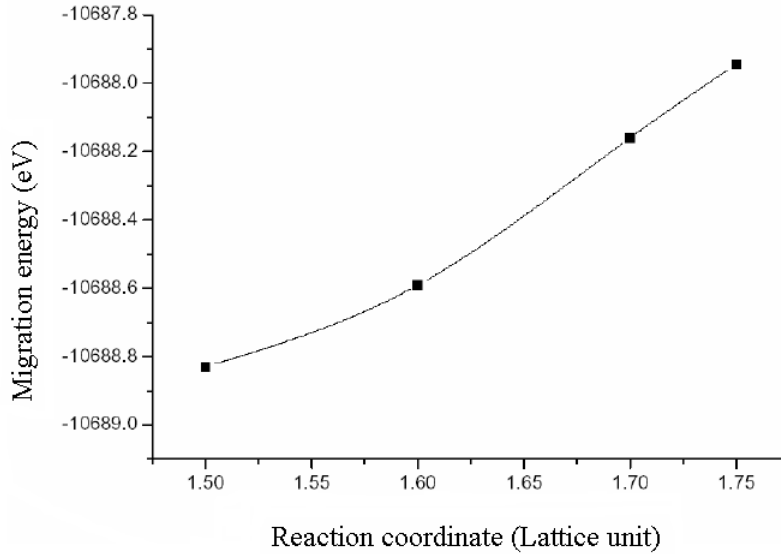


Figure 4.2: Plot of displacement versus reaction coordinate for carbon jump from octahedral to tetrahedral position at 300 K.

Therefore the diffusion of carbon from one octahedral position to the next octahedral position is energetically favorable (possible diffusion mechanism of carbon in ferrite). The migration energy of the carbon atom is the difference between energies at saddle point and the initial position in this curve. According to this the migration energy of carbon calculated is equal to 0.89 eV. This value which is calculated at room temperature is consistent with the result obtained by Derek J. Hepburn, (0.89 eV) during the potential generation using data fitting procedure [16]. That emphasizes strong dependence of the result of simulation on inter atomic potential used. The results of migration energies we obtained and reported by J. Hepburn both are in good agreement with experimentally reported values 0.83 eV [13].

The second curve (Fig 4.2) shows the migration of carbon from one octahedral position to the next tetrahedral site. During this jump the local minimum energy of the system increases and became maximum at the final position of the jump.

This jump of carbon atoms from the preferential position to the nearest neighbor tetrahedral position is not allow the stability of carbon atoms and the system as a whole and it is not energetically favorable. Activation energy as discussed in the previous section is the energy required for the jumping atom to passes through neighboring atoms. It is the sum of formation and migration energies of carbon that jumps between two successive octahedral position as given in Table 4.3. The migration energy curve given in Fig 4.3 shows temperature dependency of migration energy of carbon that increases with temperatures keeping all other factors constant.

Table 4.3: Result of migration and activation energies at room temperatures.

$Temperature (K)$	$E_{fo}(eV)$	$E_m(eV)$	$Q(eV)$
300	-6.235	0.886	-5.349

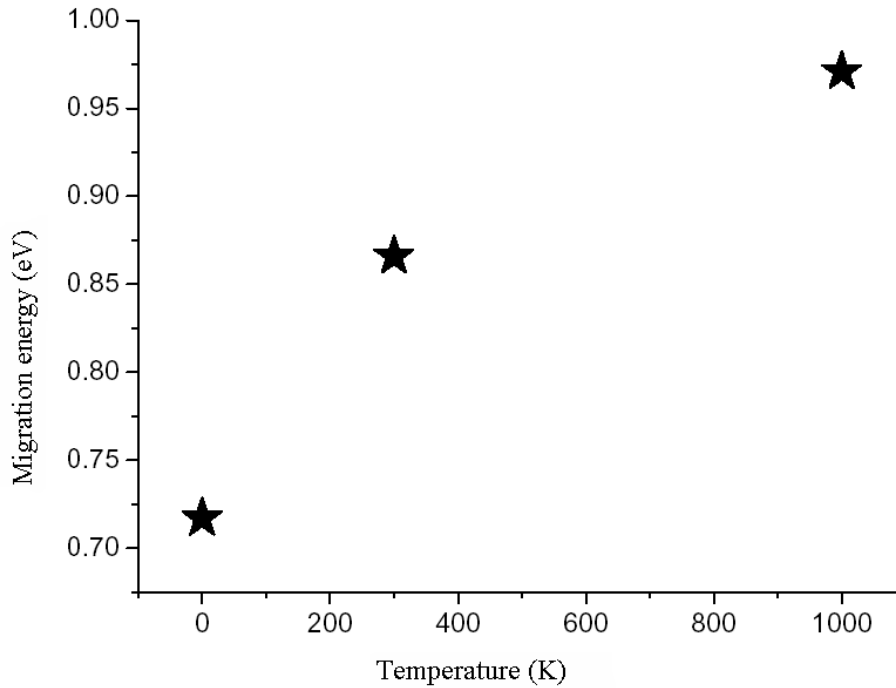


Figure 4.3: Plot of migration energy versus temperature.

4.2 Molecular Dynamics Simulation Results

The molecular dynamics simulation results of equilibrium lattice constant as a function of carbon concentration that are reported in this section are obtained by introducing all carbon atoms in the sample at the preferential positions (octahedral position) at the temperature of simulation. The corresponding equilibrium lattice parameters used are those values obtained for pure ferrite in equilibrium at specified temperature. The result of equilibrium lattice parameter for pure ferrite obtained at room temperature (2.859 Å) is slightly less than experimental values (2.870 Å). The values of equilibrium lattice constant obtained at elevated temperature 2.888 Å at 1000 k as expected increase with temperature and greater than the value at 0 k (2.855 Å).

Table 4.4: Results of equilibrium lattice constants (a) and (c) at room temperature.

<i>Carbon content wt %</i>	0.0405	0.081	0.162	0.243	0.324	0.405
$a(\text{Å})$	2.860	2.859	2.856	2.855	2.853	2.852
$c(\text{Å})$	2.860	2.862	2.870	2.872	2.875	2.877

The result of lattice parameters as a function of carbon content at room temperature is given in Table 4.4. These result shows that the values of average lattice size along the three vectors (100,010 and 001) varies equally as the amount of carbon atoms dissolved in the bulk increases up to 0.081 wt %. As the amount of dissolved carbon atoms became 0.081 wt % the average values of lattice size along the three vectors starts splitting. This splitting is due to the lattice stress that became sufficient to change the values of average size along the three vectors and one side became elongated to accommodate the excess carbon atoms introduced in the system. This distortion is martensite distortion (bcc-bct) that occurs in definite orientation of iron atoms due to preferential distribution of carbon atoms to the bcc lattice of ferrite at octahedral interstitial positions. Therefore according to our simulation this concentration of carbon (0.081 wt %) is the critical value (the minimum concentration) for structural transition of martensite to occur.

Table 4.5: Comparison of simulation results of minimum amount of carbon with experimental values at 300 K.

Result	<i>This work</i> (eV)	<i>Smith and Hasheni</i> (eV) [37]	<i>Zhong and liu</i> (eV) [11]
wt %	0.081	0.02	0.18

The deviation of our simulation results Fig 4.4 from the experimentally reported value as shown in Fig 4.5 may have different cause.

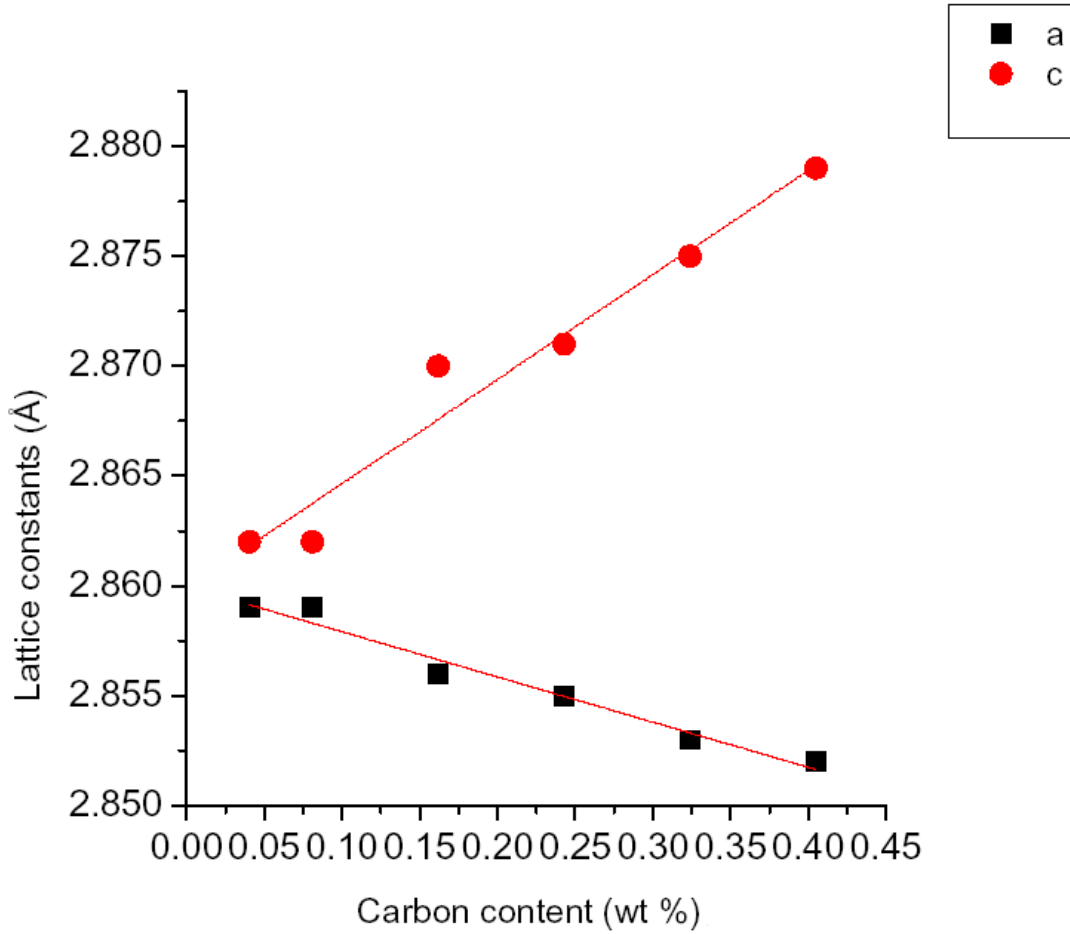


Figure 4.4: Plot of simulation result of lattice parameter versus carbon content at 300 K.

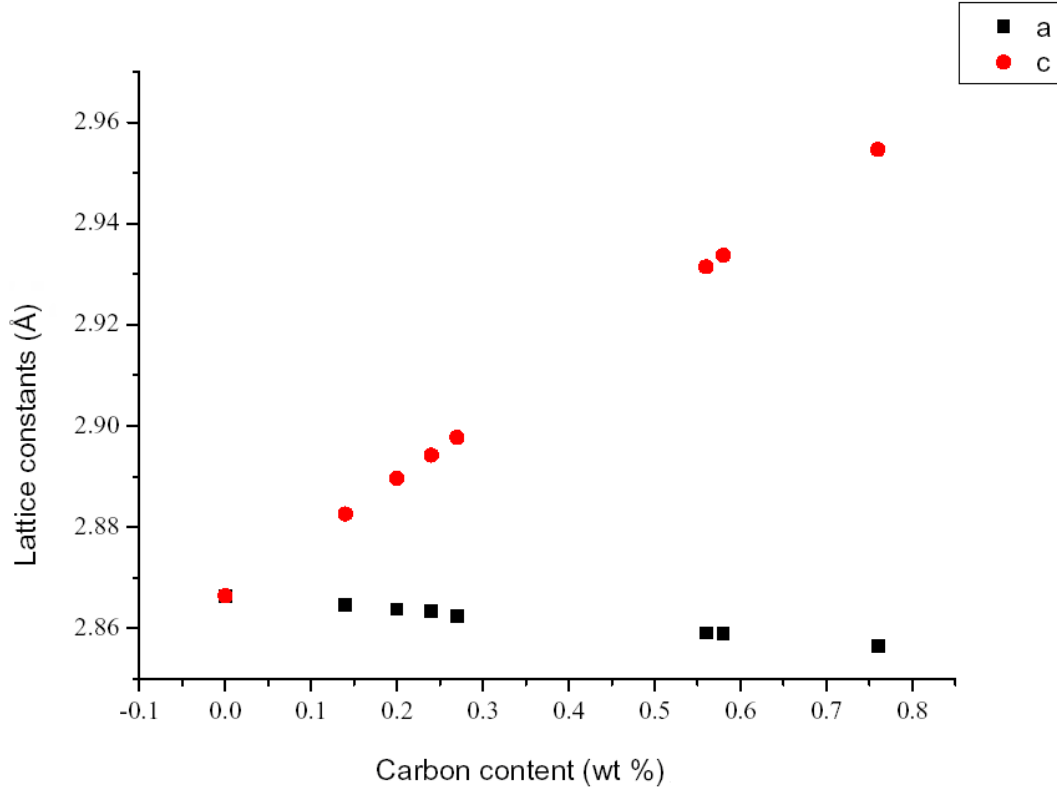


Figure 4.5: Plot of experimentally determined result lattice parameter versus carbon content at 300 K.

First this result is obtained for idealized Fe-C system that doesn't incorporate carbon-carbon interaction that could have an effect on the total energy and sizes of the system. This in turn shows strong dependence of the simulation result on the pseudo potential used. Even though there is slight discrepancy in the values of critical point the phenomena is well captured with the hypothesis that at low carbon content ferrite is cubical and becomes tetragonal (martensite) for carbon content greater than critical point. The value of critical point of carbon we obtained is consistent with the values reported by Smith and Hasheni [37] as shown in Table 4.5. Thus the embedded atom potential we used for our simulation characterized the low solubility of ferrite. Fig 4.5 shows the strong dependence of lattice parameter on temperature for fixed number of carbon content.

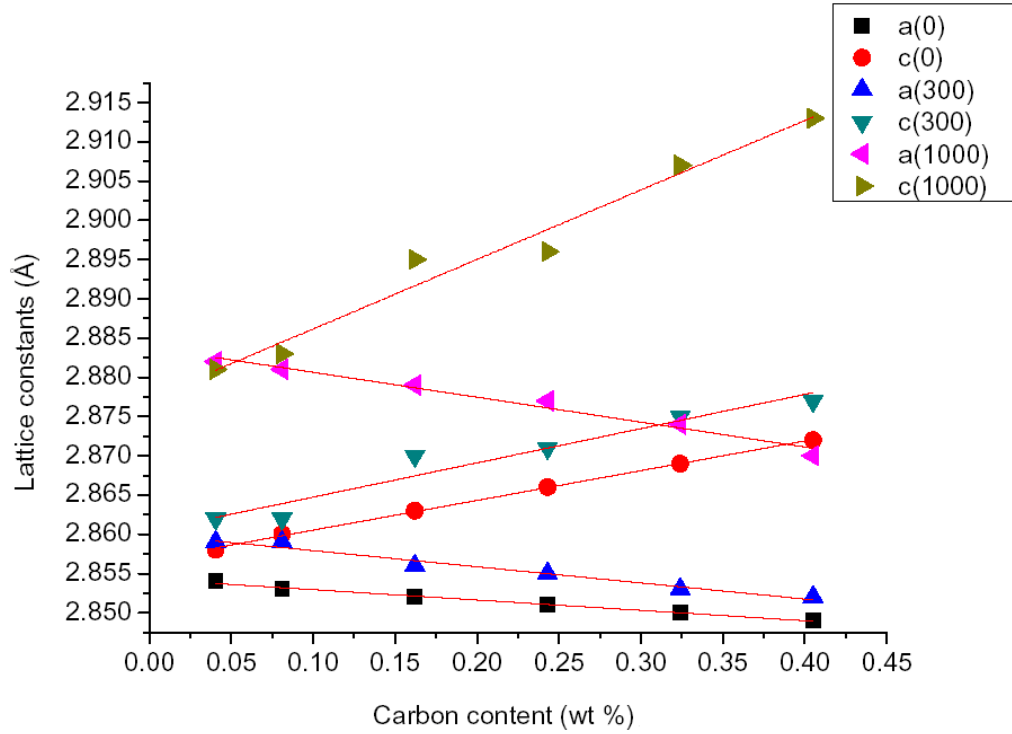


Figure 4.6: Plot of lattice parameter versus carbon content as a function of temperature.

The linearity behavior of equilibrium lattice constant with carbon content is also investigated by comparing constants (slops) of the relation between equilibrium lattice constant and carbon content. This behavior as we have discussed in Chapter one was established first by Kurdjumov [11]. According to his discussion the dependence of lattice parameter (a and c) of martensite upon carbon content are expressed linearly with the following equations:

$$c = a_0 + \alpha p \quad (4.2.1)$$

$$a = a_0 - \beta p \quad (4.2.2)$$

where p is the carbon content (wt %), a_0 is the lattice constant α and β are constants (slopes). The values of α and β in this work are approximated from the slope of the graph fitted to linearity. The comparison of the result of these constants obtained from our simulation with theoretically estimated values by Kurdjumov [11] are given in Table 4.6. As we see from this table the results are in good agreement.

Table 4.6: Results of α and β compared with theoretical value.

<i>Temperature</i>	a_0 (Å)	α (<i>theory</i>)	α (<i>thiswork</i>)	β (<i>theory</i>)	β (<i>thiswork</i>)
0 K	2.866	-	0.0378 ± 0.00056	-	0.0131 ± 0.00058
300 K	2.855	0.116 ± 0.002	0.0512 ± 0.005	0.013 ± 0.002	0.02226 ± 0.0018
1000 K	2.888	-	0.089 ± 0.006	-	0.0306 ± 0.0031

Diffusion constant of carbon in the bulk of ferrite is computed from mean square displacement as described in Chapter three. In this method the simulation is repeated hundred times until the system equilibrate as shown in Fig 4.6 and the square of the mean value of these displacement is calculated.

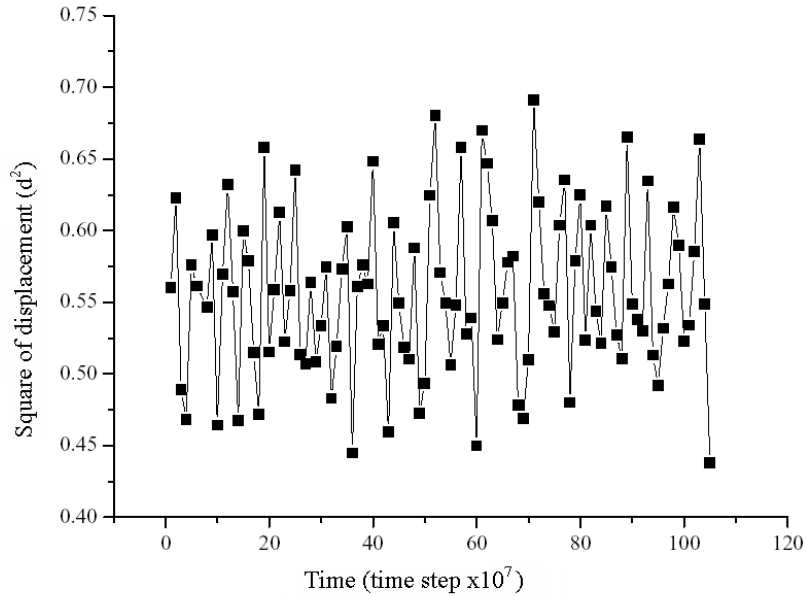


Figure 4.7: Plot of square of displacement versus time at 300 K.

The diffusion constant of carbon we calculated from mean square displacement is used to compute diffusion coefficient using Eq. 3.2.1. The diffusion coefficient calculated in this work $9.736 \times 10^{-8} m^2/s$ is close to the value $2.13 \times 10^{-7} m^2/s$ reported by C. Domain [38]. Due to the importance of activation energy and long residential time for diffusion constant calculation, this value of a MD study of diffusion constant stress their dependence on the inter-atomic potential used.

4.3 Molecular Static Simulation Results in Martensite

The diffusion characteristic results of carbon in martensite for the critical concentration of carbon (maximum solubility of ferrite) reported in this section is obtained under molecular static frame work. Formation energies are computed as before for a single carbon introduced at t-sites and o-sites keeping all other atoms at their preferential position. The result of formation energy at critical point is shown in Table 4.7.

Table 4.7: Results of formation energies of carbon in martensite.

<i>Energies (eV)</i>	E_p (eV)	E_t (eV)	E_o (eV)	E_{fo} (eV)	E_{ft} (eV)
–	-10579.369	-10743.760	-10744.690	-125.120	-124.189

Table 4.8: Results of migration energies of carbon in ferrite and martensite parallel and perpendicular to c-axis.

<i>jump direction</i>	<i>in marteinsite</i>	<i>in ferrite</i>
<i>parallel</i>	1.45	0.866
<i>perpendicular</i>	1.06	0.866

This result again shows the preference of octahedral position to be occupied by carbon atoms at equilibrium. That means the diffusion of carbon atom in both ferrite and transformed martensite are the jump from one preferential position to the next nearest neighbor preferential position. Hence ferrite-martensite structural transformation is not driven by diffusion. Instead concentration based strain developed around iron atoms is the deriving force responsible for such structural transition to occur. Unlike ferrite the migration energy of carbon in martensite parallel and perpendicular to the c-axis as shown in Fig 4.7 are different. Its migration energy parallel to the c-axis that is in the direction of stretching or deriving force is greater than the one obtained in the direction perpendicular to the c-axis. This is due to the reduction of interaction force or potential barrier among atoms as a result of stretching. The effect of deriving force during transition can also be another factor that affect the migration energy of carbon.

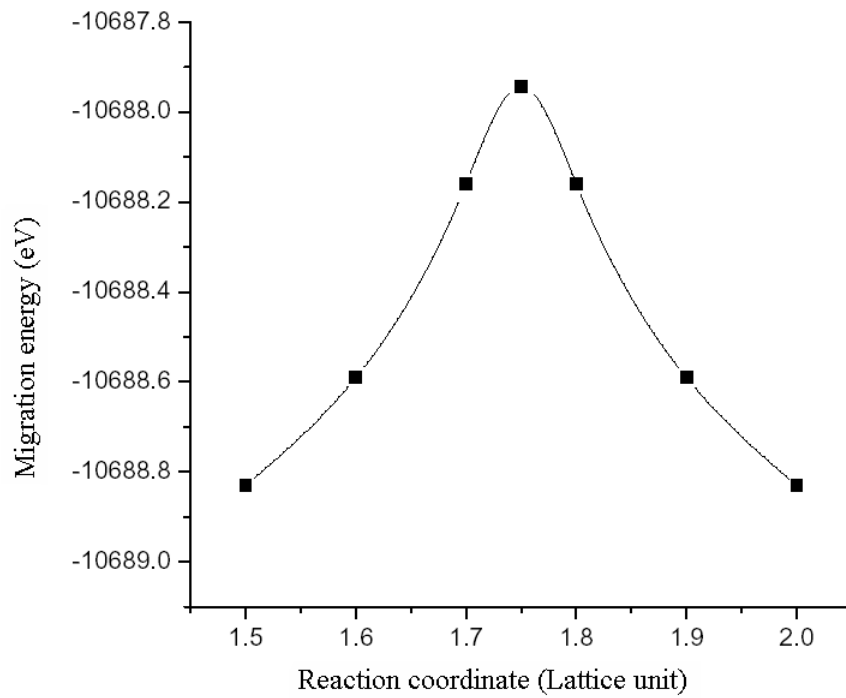
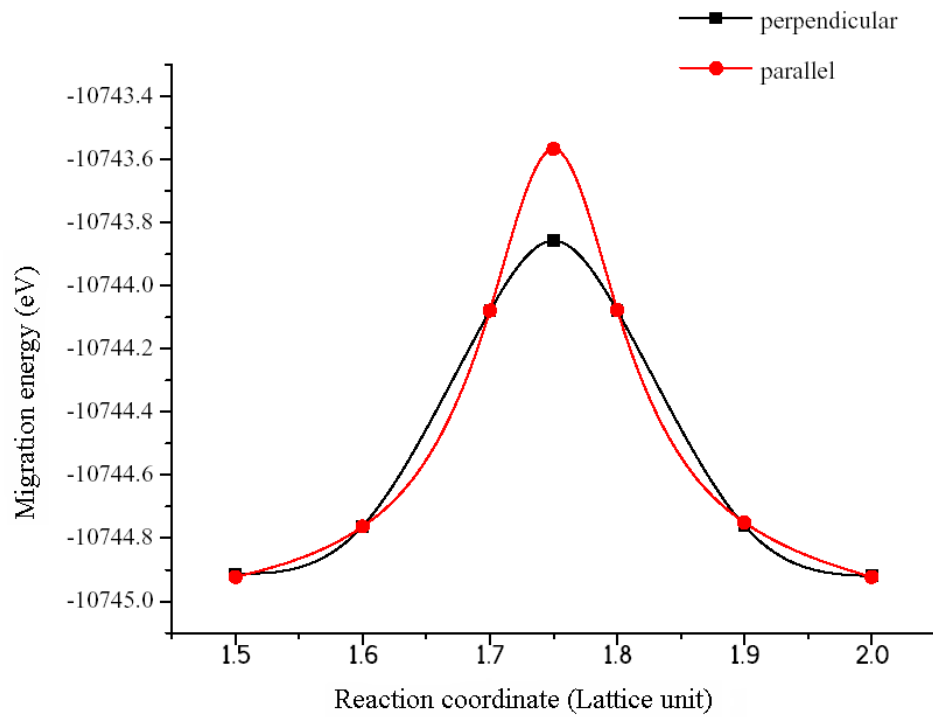


Figure 4.8: Migration energy curve of carbon in martensite and ferrite.

Chapter 5

Summary And Conclusion

Structural transformation of martensite with increasing number of carbon content and properties of carbon diffusion are investigated using molecular static and molecular dynamic simulation. For both simulations the atomic interaction was described by embedded atom potential generated by Derek J. Hepburn and Graeme J. Ackland. From molecular static simulation of formation energies octahedral position is found as the preferential position with minimum energy occupied by carbon atom introduced in ferrite. The other interstitial site, tetrahedral position has been found to be the transition site of carbon that jumps between adjacent octahedral positions. This tetrahedral site exactly corresponds to the saddle point of carbon migration. Both the formation and migration energy calculated in this simulation is consistent with Ab initio simulation result reported [18]. The temperature dependence analysis of these results shows that the migration energy increased with temperature. But to do similar simulation and reach to the same conclusion in martensite the values of formation and activation energies should be calculated for more carbon atom found in the solution. In addition since this values in ferrite were obtained for single carbon atom introduced assuming none interacting defect, the situation could be complex and different as the concentration increases. Therefore we believe that this analysis requires the existence of multiple interstitial configurations and pseudo potential that can describe atomic interaction between carbons and iron for increasing number of carbon at elevated temperature.

In this study using EAP we found that the critical point of transition (0.081 wt %) which is less than the one obtained experimentally (0.18 Wt %). Hence experimental complexity to determine the critical point (splitting of lattice parameters) of carbon at very low concentration can be resolved using computer simulation for good potential that can describe atomic interaction perfectly. The diffusion coefficient of carbon was also determined effectively with molecular dynamic simulation. Even though experimental complexity of diffusion coefficients calculation are resolved using molecular dynamics simulation, it is found computationally expensive and demands potential that can describe interaction among defects. From the results of both simulation martensite transition is found to be concentration driven diffusionless transition that occurred by cooperative small displacements of all atoms in structure. Thus computer simulation is very useful to estimate the concentration of carbon in supersaturated alpha phase of steel. Finally the embedded atom interatomic potential we used in this simulation gives in general a reasonably good description of properties in ferrite and martensite. This conclusion is related to both static properties (formation and migration energies) as well as dynamics (diffusion coefficient and lattice parameters).

References

- [1] R. W. Siegel, J. Nucl. Mater. 69 and 70, 117 (1978).
- [2] N.Sijakov, G. Kurdjumov, and N.Gouf Dob, Z.Phys. 45, 384 (1927).
- [3] C.zener, Phys.Rev.74, 639 (1948).
- [4] G.V. Kurdjumov and E.Kaminsky, Z.phys. 53, 696 (1929.)
- [5] G. kurdjumov and A.G Khachaturan, Acta Metall. 23 1077 (1975).
- [6] G.Hagg, J.iron steel.inst.London 130,439 (1934).
- [7] E.Ohman, J. Iron steel Inst. London 123,445 (1931).
- [8] K.Honda and Z.Nishiyama, Trans. Am. Soc. Steel Treat, 20, 464 (1932).
- [9] G.Kurdjumov and E.Kamisky, j.Iron steel Inst. London 195,26 (1960).
- [10] P.G.Winchell and M.cohen, Trans. Am.soc.Met.55, 347 (1962).
- [11] L.Xiau,Z.Fan and Z.Jinxu Physical Review B 52, 9970 (1995).
- [12] J.L.Bonnetien and J. Bigot, Mater. Trans. 41, 78 (2000).
- [13] D.E. Jiang and E.A.Carter Physical Review B 67, 214103 (2003).
- [14] P.G. Winchell and M.cohen, Trans. Am. soc. Met. 55, 347 (1962).
- [15] G.V.Kurdjumov and G.Sachs, Z. Phys. 64,325 (1930).
- [16] D. J. Hepburn and G.J. Ackland, Phys. Rev. B 78, 165115 (2008).
- [17] V. Rosato, Acta Metall. 37, 2759 (1989).

- [18] Timothy T. Lau, Clemens J. Forst, Xi Lin, Julian D. Gale, Sidney Yip, and Krystyn J. Van Vliet. *physical Review lett.* 98, 215501 (2007).
- [19] J. P. Perdew, K. Burke, and M. Ernzerhof, *Phys. Rev. Lett.* 77, 3865 (1996).
- [20] F.W.Finnis and J.E Sinclair, *philos. Mag.A* 50, 45 (1985).
- [21] M. Ruda, D. Farkas, and J. Abriata, *Scr. Mater.* 46, 349 (2002).
- [22] N. Metropolis, A. W. Rosenbluth, M. N. Rosenbluth, A. H. Teller, and E. Teller, *J. chem. Phys.* 21, 1087 (1953).
- [23] B. J. Alder and T. E. Wainwright, *J. Chem. Phys.* 27, 1208 (1957).
- [24] J. E. Sinclair and R. Fetcher, *J.Phys C*, 7, 864 (1972).
- [25] W. G. Hoover, *Lecture Note in Physics: Molecular Dynamics*, edited by H. Arita, Kyoto, J. Ehlers, Mnchen, K. Hepp, Zrich, R. Kippenhahn, Mnchen, H. A. Weidenmller, Heidelberg, and J. Zittartz, Kln, page13, Springer-Verlag, (1986).
- [26] J. M. Haile, *Molecular Dynamics Simulation Elementary Methods*, page 40-42, Wiley-Interscience (1992).
- [27] Large-scale Atomic/Molecular Massively Parallel Simulator. <http://lammmps.sandia.gov> - Sandia National Laboratories.
- [28] M.C Holian, *Molecular Physics*, 78, 533-44 (1993).
- [29] W. G. Hoover, *Physical Review A* 31,3 (1984).
- [30] W. G. Hoover *Physical Review A* 34,3(1986).
- [31] B. Sepiol, C. Czihak, A. Meyer, G. Vogl, J. Metge, and R. Rffer, *Hyperfine Intereaction*, 113, 449 (1998).
- [32] M.s Daw and M.I Baskes, *Phys.Rev.Lett* 50, 1285 (1983).
- [33] J. E. Sinclair and R. Fetcher, *J. Phys C*, 7,864 (1972).
- [34] H. Hohenberg and W. Kohn, *Physical Review*, 136, 13864 (1964).

- [35] E.Clemen and C.Roeti,At,Data Nucl.Data table 14,177(1974).
- [36] J. Rose, J. Smith, and J. Ferrante, Physical Review B, 28, 1835 (1983).
- [37] S. William F. Hashemi, Javad (2006), Foundations of Materials Science and Engineering, 4th edn, McGraw-Hill, ISBN 0-07-295358-6, pp. 388-391.
- [38] C. Domain C. S. Becquart and J. Foct Physical Review B 69, 144112 (2004).

Declaration

This thesis is my original work and has not been presented for a degree in any other University, and that all the sources of material used for the thesis have been duly acknowledged.

Yilma Mengistu

Place and time of submission: Addis Ababa University, January 2011

This thesis has been submitted for examination with my approval as University advisor.

Dr. Mulugeta Bekele

(Advisor)
